Electronic Supplementary Information

Combining plasmonic trap filling and optical backscattering for highly efficient third generation solar cells

Chen Wang,[a] Chang Li,[a] Shanpeng Wen,*[a] Pengfei Ma,[a] Yang Liu,[b] Roderick C. I. MacKenzie,*[c] Wenjing Tian[b] and Shengping Ruan[a]

a) State Key Laboratory on Integrated Optoelectronics and College of Electronic Science & Engineering, Jilin University, Changchun 130012, P. R. China

b) State Key Laboratory of Supramolecular Structure and Materials, Jilin University, Changchun 130012, P. R. China

c) Faculty of Engineering, The University of Nottingham, University Park, Nottingham, NG7 2RD, UK

*Corresponding authors: sp_wen@jlu.edu.cn; Roderick.Mackenzie@nottingham.ac.uk

Synthesis of AuNRs

The AuNRs were prepared according to the seed-mediated growth method, reported by EI-Sayed and co-workers.[1] Firstly, a seed solution was prepared by mixing 7.5 mL of CTAB (0.1 M), 2.5 mL of $HAuCl_4$ (1 mM) and 0.6 mL of ice-cold $NaBH_4$ solution (10 mM) under vigorously stirring at 27 °C. After 2 hours, the seed solution was used for the synthesis of the AuNRs. Secondly, 66 mL of 0.1 M CTAB was mixed with 60 mL of 1 mM $HAuCl_4$ in a 250 mL flask, then 0.6 mL of 0.01 mM silver nitrate aqueous solution and 0.55 mL of 2 M hydrochloric acid were added to the flask. After gently stirring the solution to 2 hours, 0.96 mL of 0.1 M Ascorbic Acid and 1 mL of the as-synthesized seed solution were simultaneously added to initiate the growth of the AuNRs. These NRs were aged for 5 hours to ensure full growth at 27 °C. Finally, excess CTAB was removed by centrifuging at 12000 rpm for 15 min, and highly concentrated AuNRs colloid solution was obtained.
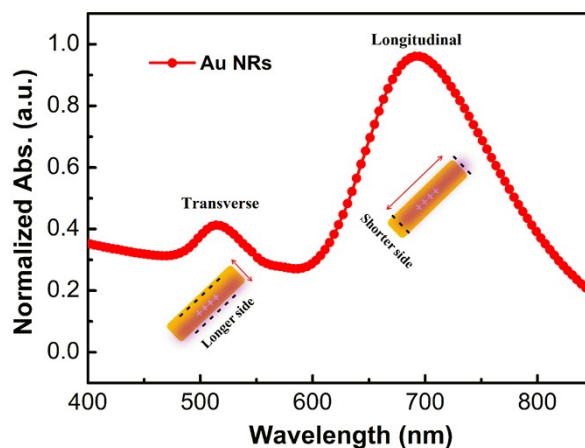
Fig. S1. The absorption spectrum of as-prepared AuNRs.

Device fabrication and characterization

The basic device structure is ITO/PEDOT:PSS/PTB7:PC$_{71}$BM/ZnO/Al. ZnO nanoparticles (NPs) were prepared as published elsewhere.[2] It should be noted that small amount of ethanolamine (0.2 wt%) was added into ZnO methanol dispersion and 30 min ultrasonic treatment was applied to obtain cluster free ZnO NPs solution. Then, the ZnO solutions doped with different concentration of AuNRs were prepared by adding highly concentrated AuNRs colloid into ZnO solution, followed by ultrasonic treatment for 30 min before use. The patterned ITO glass substrates (15 ohm/square) were pre-cleaned by ultrasonic baths in detergent, deionized water, acetone and isopropyl alcohol sequently. After UV-Ozone treatment for 10 min, The PEDOT:PSS (Clevious P VP AI 4083) solutions were spin-coated (5000 rpm) onto the ITO substrates at a thickness of ~ 40 nm (after passing through a 0.22 μm filter). Then the substrates were annealed at 140 °C for 30 min in air and transferred into a nitrogen-filled glove box. Blend solution for the active layer was prepared by dissolving PTB7 and PC$_{71}$BM (1:1.5 w/w) in chlorobenzene/1, 8-diiodooctane mixed solvent (97:3 v/v) with a concentration of 10 mg/mL for PTB7 polymer. The blend solution was stirred in glove box for 24 h before film casting. The PTB7:PC$_{71}$BM active layer can be obtained by spin-coating the aforementioned blend solution at 1400 rpm for 45 s on top of the PEDOT:PSS film (after passing through a 0.45 μm filter) and then placing the substrates inside a vacuum antechamber for 2 hours. The active layer thickness is ~ 95 nm, which was measured by the Veeco DEKTAK 150 surface profilometer. Then the prepared ZnO solutions (without and with Au NRs) were immediately dropped and spin-coated onto the active layer at the speed of 2000 rpm to form ZnO

rear side transporting layer with the thickness of around 35 nm. The devices were finally completed by thermal evaporation of a 100 nm thick aluminum cathode in vacuum (vacuum degree $\approx$ 5×10^{-4} Pa) with a shadow mask (device active area of about 0.064 cm^2). The current density-voltage (*J-V*) characteristics of fabricated devices were measured using Keithley 2400 Source Meter in the dark and under Air Mass 1.5 Global (AM 1.5 G) solar illuminations with an Oriel 300 W solar simulator intensity of 100 mW/cm^2 (denoted as 1 sun). The light intensity was measured by a photometer (International light, IL1400) and corrected by a standard silicon solar cell. Before recording *J-V* curves, the device were placed on weakened light irradiation (0.3 sun) equipped with UV cut filter (UV cut 410 nm) for 5 min as pre-illumination. Transmission electron microscopy (TEM) was conducted using a Hitachi H-800 electron microscope at an acceleration voltage of 200 kV with a CCD camera. The surface morphologies were characterized with atomic force microscopy (AFM, Veeco Dimension 3100). The EQE spectra were conducted using, Crowntech QTest Station 1000 AD. The UV-vis absorption and normal incident reflection spectra were taken using Shimadzu 3600 UV−visible-NIR spectrophotometer.
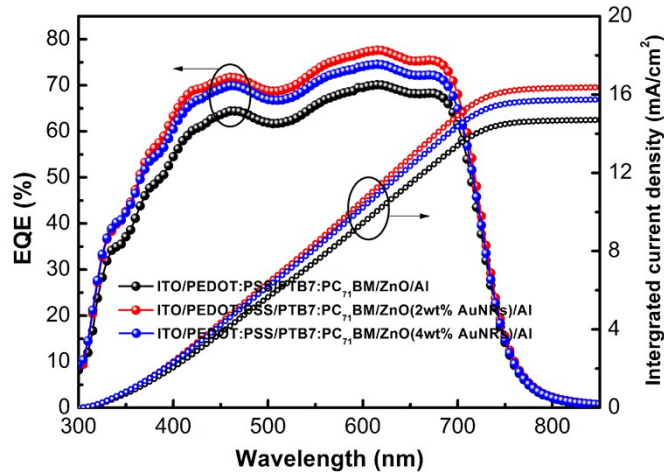
**Fig. S2** EQE spectra of reference and plasmonic devices.

Determining carrier mobility by SCLC method

As for SCLC measurements, the dark *J-V* characteristics were plotted on a log scale and fitted to a space charge limited form, where the SCLC is described by the following equation:

$$J = \frac{9}{8}\varepsilon_0\varepsilon_r\mu_0\frac{(V-V_{bi})^2}{L^3}exp\left\{0.89\beta\sqrt{\frac{V-V_{bi}}{L}}\right\}$$

, where ε_0 is the permittivity of free space (8.85×10^{-12} F m^{-1}), ε_r is dielectric constant of the polymer, typically this constant is assumed to be 3, μ_0 is the hole or electron mobility, V_{bi} is the built-in voltage due to the work function difference of electrodes and L is the thickness of active layer.

In order to obtain more supportive evidence to confirm that AuNRs-generated hot carriers fill trap state of ZnO and lead to a high mobility, we compared electron mobility of device with AuNRs before and after pre-illumination as shown in Fig. S3. It can be seen that mere incorporation of AuNRs didn't clearly improve the electron mobility of device, only after pre-illumination the device with the Au-NRs has a higher mobility.
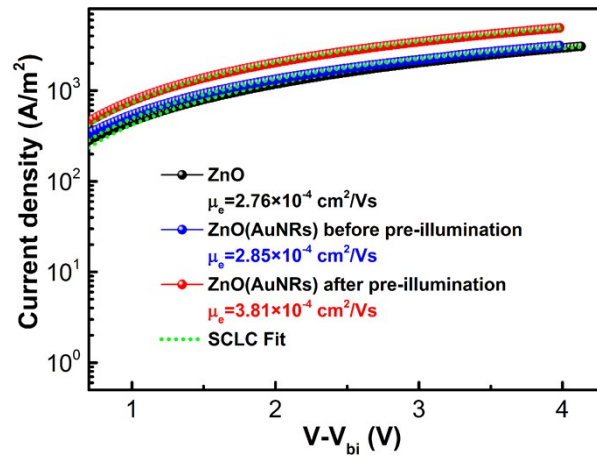
Fig. S3 The dark *J-V* characteristics of electron-only devices before and after pre-illumination.

Photo-CELIV and TPC measurements

For TPC measurement, the samples were irradiated through the ITO side by one 10 ns 532 nm laser pulse (Continuum Minilete TM Nd:YAG) with the different energy flux ranging from 1.0-96.8uJ/cm^2, the photocurrent was recorded on an oscilloscope (Tektronix MSO 4054) by measuring the voltage drop over a 50 ohm sensing resistor in series with the solar cell. In photo-CELIV measurement, the devices were irradiated through the ITO side by one 10 ns 532 nm laser pulse with the energy flux of 96.8uJ/cm^2. After a variable t_{del}, a linear extraction ramp was applied via a function generator. The ramp was 100 μs long and 2 V in amplitude.
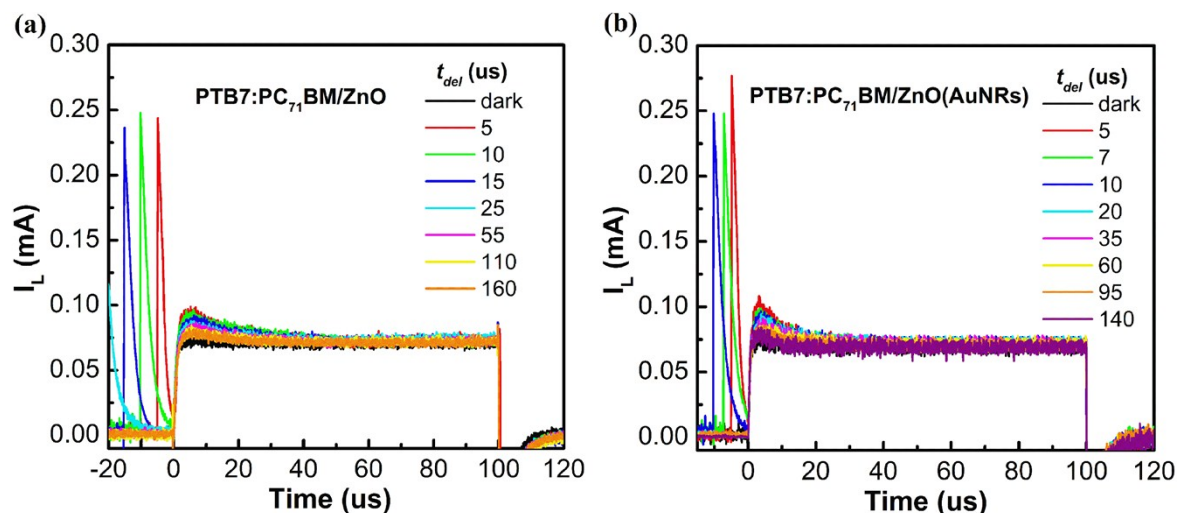
Fig. S4 Part of photo-CELIV transients of OSCs without (a) and with AuNRs (b) for different t_{delay}.

### Storage lifetime test of the organic solar cells

We have therefore re-measured the efficiency of a series of devices with and without the 2 wt% AuNRs. These devices were un-encapsulated, measured in ambient conditions but stored in dark in glove-box between measurements. The results have been plotted in the following Fig. S5.
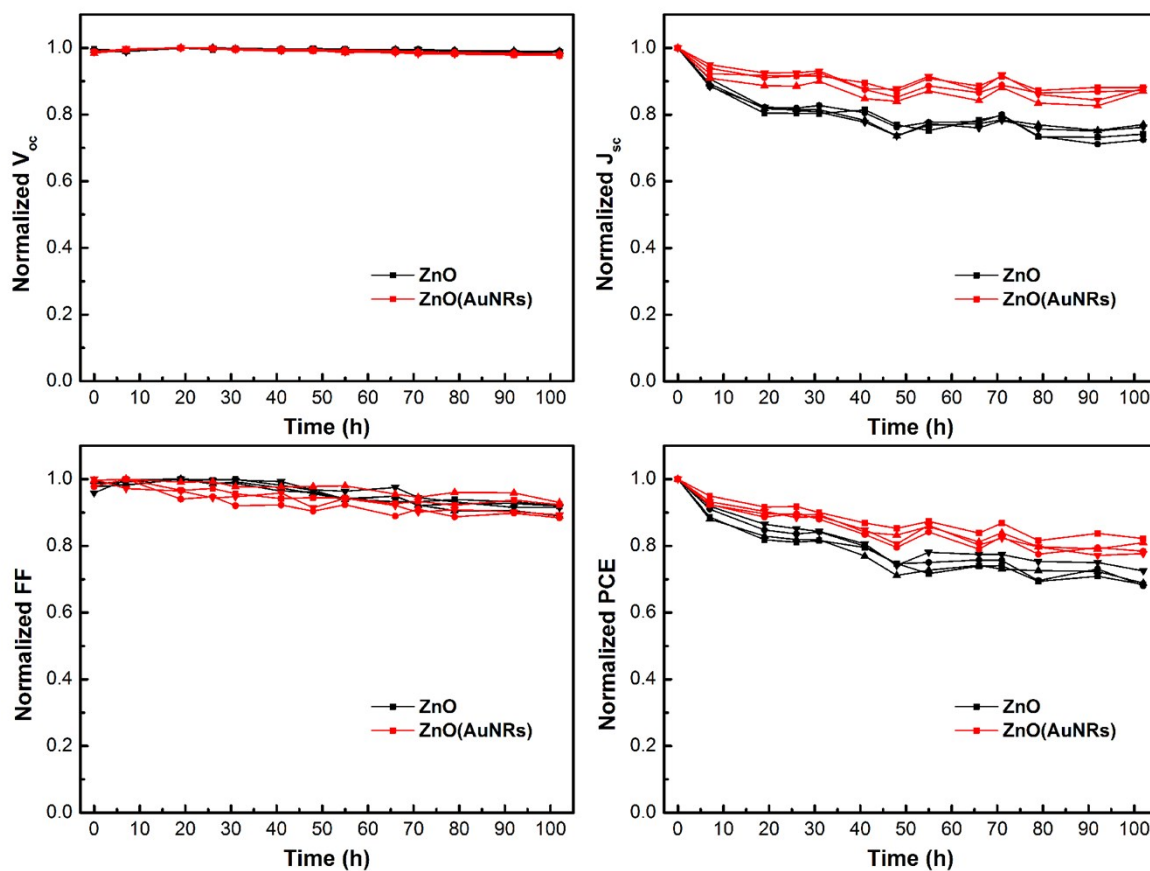
**Fig. S5** Aging of ZnO and ZnO(2wt% AuNRs) based devices.

The effect of the ZnO layer on the photon distribution within the device

When the refractive index or absorption of any layer in the device is changed, for example by adding nanorods to the ZnO matrix, there is a possibility that the modal distribution of light in the device could change and this could be the reason for the change in efficiency of the device. To rule this out, we first measured the real and imaginary parts of the refractive index of the ZnO layer with and without the nanorods, and the complex refractive index of the active layer. The complex refractive indices for the other layers were taken from the literature. Then by solving the forward and backward propagating wave equations within the sandwich structure of the device for over the AM 1.5 solar spectrum, we were able to calculate the distribution of absorbed photons within the device. This is depicted in Fig. S6. The difference in the photon density caused by the addition of nanorods to the ZnO layer was found to be negligible (only around 1.4% in the active layer). Thus, the increase in device efficiency cannot be explained by the changes in the refractive index of the ZnO layer alone, further supporting the hypothesis that the observed increase in device efficiency is due to plasmonic effects.
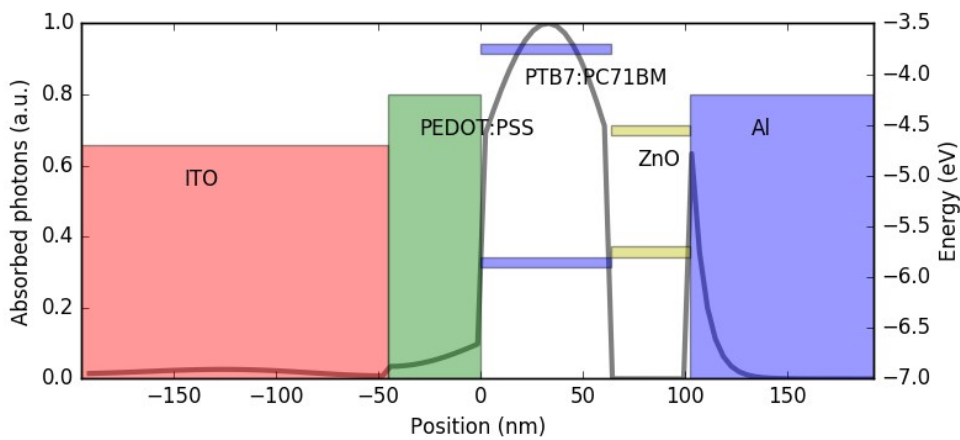
Fig. S6: The distribution of absorbed photons within the device. The addition of the nanorods to the ZnO led only a 1.4% increase in the average photon density within the active layer. This is not enough to account for the increase in device efficiency, we can therefore rule out a change in the photon distribution within the device as being the root cause of the increase in device efficiency.

The diagram of plasmon-induced hot-electrons formation and charge transfer processes.
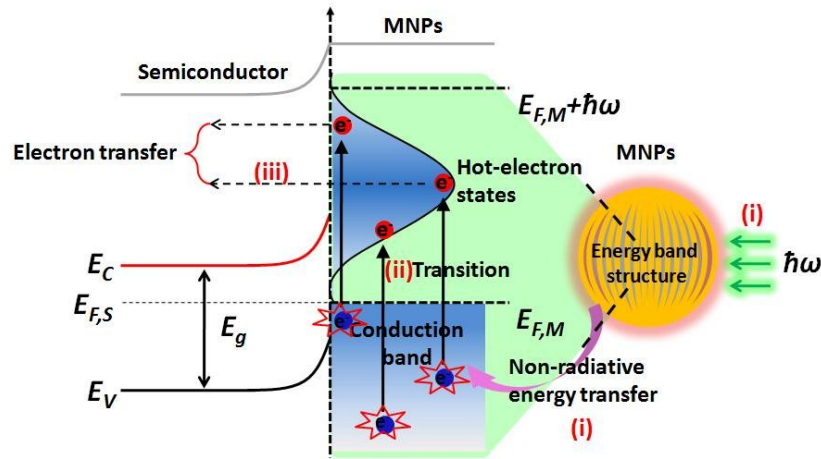
Fig. S7: i) Excitation of LSPR modes and then LSPR non-radiatively decays via transferring the collected electromagnetic energy ($\hbar\omega$) to conduction band electrons of MNPs; ii) The conduction band electrons absorb this part of transferred energy and are excited from different occupied energy levels (over the entire DOS distribution) to above the Fermi energy (E_F) level This creates a broad hot-electron states distribution possessing the energy region of $E_F < \varepsilon < E_F + \hbar\omega$,[3-4] iii) at the MNP/semiconductor interface a Schottky junction is formed. Those hot-electrons with sufficient energy may overcome the Schottky barrier, transfer to the nearby semiconductor and contribute to photocurrent.[5-6]

Reference

[1] X. Huang, I. H. El-Sayed, W. Qian and M. A. El-Sayed, *J. Am. Chem. Soc.*, 2006, **128**, 2115.

[2] W. J. E. Beek, M. M. Wienk, M. Kemerink, X. Yang and R. A. J. Janssen, *J. Phys. Chem. B*, 2005, **109**, 9505.

[3] S. Linic, P. Christopher and D. B. Ingram, *Nat. Mater.*, 2011, **10**, 911.

[4] C. Clavero, *Nat. Photon.*, 2014, **8**, 95.

[5] Y. Tian, X. Shi, C. Lu, X. Wang and S. Wang, *Electrochem. Commun.*, 2009, **11**, 1603.

[6] Y. Tian and T. Tatsuma, *Chem. commun.*, 2004, **16**, 1810.